Sensor and Simulation Notes
Note XLVII
9 August 1967

The Diffraction of an Electromagnetic Plane Wave at a Bend in a Perfectly Conducting Planar Sheet

Capt Carl E. Baum
Air Force Weapons Laboratory

Abstract

One way to launch an approximate electromagnetic plane wave on a parallel plate, cylindrical transmission line is to use a conical transmission line with a similar cross section. Such a match is not perfect. Part of the problem of this match can be approximately treated by considering the diffraction of an electromagnetic plane wave at a bend in a perfectly conducting sheet which is taken infinite in extent. The solution for the magnetic field for an incident step function wave is obtained as a special case of a problem solved by Keller and Blank involving the diffraction at a wedge. The solution is then generalized to include the electric field components. The distortion of the incident waveform is least for the smallest angle of bend in the conducting sheet.

Foreword

The graphs summarizing the diffraction of a step-function electromagnetic plane wave are grouped together at the end of section III.

We would like to thank Mr. Ralph Powell and Mr. Ronald Thompson for the numerical calculations and the resulting graphs.

I. Introduction

One way to launch a plane wave on a cylindrical transmission line is to use an appropriately matched conical transmission line.[1] Such a match is only approximate, but it can be improved by lengthening the conical transmission line. This makes the spherical wavefront on the conical transmission line more nearly approximate the desired planar wavefront on the cylindrical transmission line. In transitioning between the conical and cylindrical transmission lines, the conductors are bent through some angle. This angle can also be decreased by lengthening the conical transmission line. Nevertheless, the transition is not perfect and some distortion of the wave is introduced at the position that the conical and cylindrical transmission lines are joined.

In this note we consider part of the distortion problem by calculating the diffraction of a uniform electromagnetic plane wave which is propagating parallel to a perfectly conducting planar sheet when the wave encounters a bend in this sheet. The straight line along which the bend occurs is assumed perpendicular to the direction of propagation of the incident wave. Actually the wavefront on a conical transmission line is spherical; the use of a plane wave for the calculations is somewhat approximate. Note that there are various possible geometries for the cross sections of conical and cylindrical transmission lines using conducting wires, sheets, etc. The present calculations only apply to those types of transmission lines which use flat sheets for the conductors or other configurations which approximate flat conducting sheets to some degree. In such transmission lines the conducting sheets are not of infinite width and the wave is not uniform. Furthermore, there can be more than one conducting sheet so that there can be multiple reflections in the transmission line. The present calculations then approximate the electromagnetic fields near the bend in the conducting sheet for times before other disturbances can influence the results. For the present calculations we assume an incident step-function wave; the results can be applied to other waveforms by the use of the convolution integral.

Diffraction of a plane wave at a bend in a conducting sheet is a special case of the diffraction of a plane wave at a wedge considered by Keller and Blank.[2] Although Keller and Blank consider a scalar wave, it still applies to the present problem because there is only one component of the magnetic field to consider and this component obeys the scalar wave equation. Choosing a particular direction of incidence for the wave, the diffraction at a conducting wedge is the image problem corresponding to the diffraction at a bend in a conducting sheet. The two components of the electric field are also calculated from the magnetic field using one of Maxwell's equations.

---

1. Capt Carl E. Baum, Sensor and Simulation Note XXXI, The Conical Transmission Line as a Wave Launcher and Terminator for a Cylindrical Transmission Line, Jan. 1967.
2. J.B. Keller and A. Blank, Diffraction and Reflection of Pulses by Wedges and Corners, Comm. on Pure and Applied Math., vol. 4, p. 75, 1951.

II. Diffraction at a Perfectly Conducting Wedge

Consider then one of the cases from reference 2 as illustrated in figure 1. A perfectly conducting wedge has its edge on the z axis. The half angle of the wedge is ϕ_o. An incident step function wave (figure 1A) is propagating in a direction perpendicular to the z axis and at an angle, ϕ_1, with respect to the x axis. The magnetic field has only a z component. We define a normalized magnetic field as $h \equiv 0$ in front of the wavefront and as $h \equiv 1$ behind the wavefront. The wave propagates at a speed, c, and the time, $t = 0$, is defined by the arrival of the incident wave at the edge of the wedge, $(x,y) = (0,0)$. The boundary condition on the surface of the wedge for the single magnetic field component is that its normal derivative be zero. We also constrain that $0 < \phi_1 < \phi_o$. Note that only the case of a nonconducting medium is assumed for $\phi_o < \phi < 2\pi - \phi_o$.

After the wave has reached the wedge ($t>0$) the spatial distribution of the wave is as illustrated in figure 1B. There are regions where the incident wave has not reached, in which case $h = 0$. Where the incident wave has reached, but reflections from the wedge have not reached, then $h = 1$. Where the incident wave plus a reflection from the wedge have reached, but no reflection or diffraction from the edge of the wedge has reached, then $h = 2$. Finally, there is the region bounded by the surface of the wedge and a circle of radius, ct, centered on the origin. Inside this region the solution for h is much more complicated. Note that the radius, ct, is just the maximum distance that the diffracted fields from the edge of the wedge have reached. Inside this radius the fields are solved by using the boundary condition that h is continuous across the circular boundary. Such continuity exists because the diffracted fields which reach $r = ct$ from the edge of the wedge come from a surface of zero area The boundary conditions used are for $\phi = \pm\phi_o$ and $0 < r \leq ct$ then

$$\frac{\partial h}{\partial n} = 0 \tag{1}$$

for $\phi_o < \phi < \phi_o + \phi_2$ and $r = ct$ then

$$h = 2 \tag{2}$$

for $2\pi - (\phi_o + \phi_3) < \phi < 2\pi - \phi_o$ and $r = ct$ then

$$h = 2 \tag{3}$$

and for $\phi_o + \phi_2 < \phi < 2\pi - (\phi_o + \phi_3)$ and $r = ct$ then

$$h = 1 \tag{4}$$

The special angles, ϕ_2 and ϕ_3, are given by

$$\phi_2 = \phi_o - \phi_1 \tag{5}$$

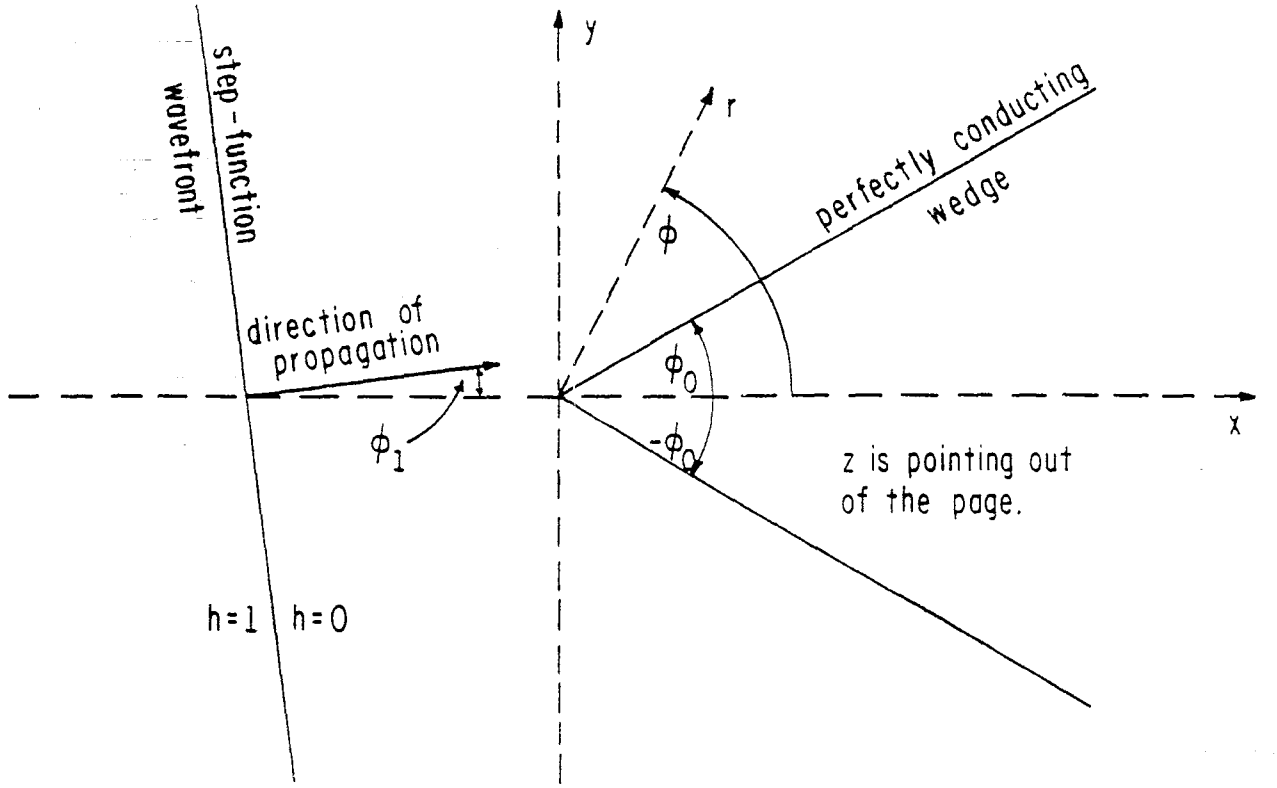

A. BEFORE WAVE INCIDENCE AT EDGE: $t<0$

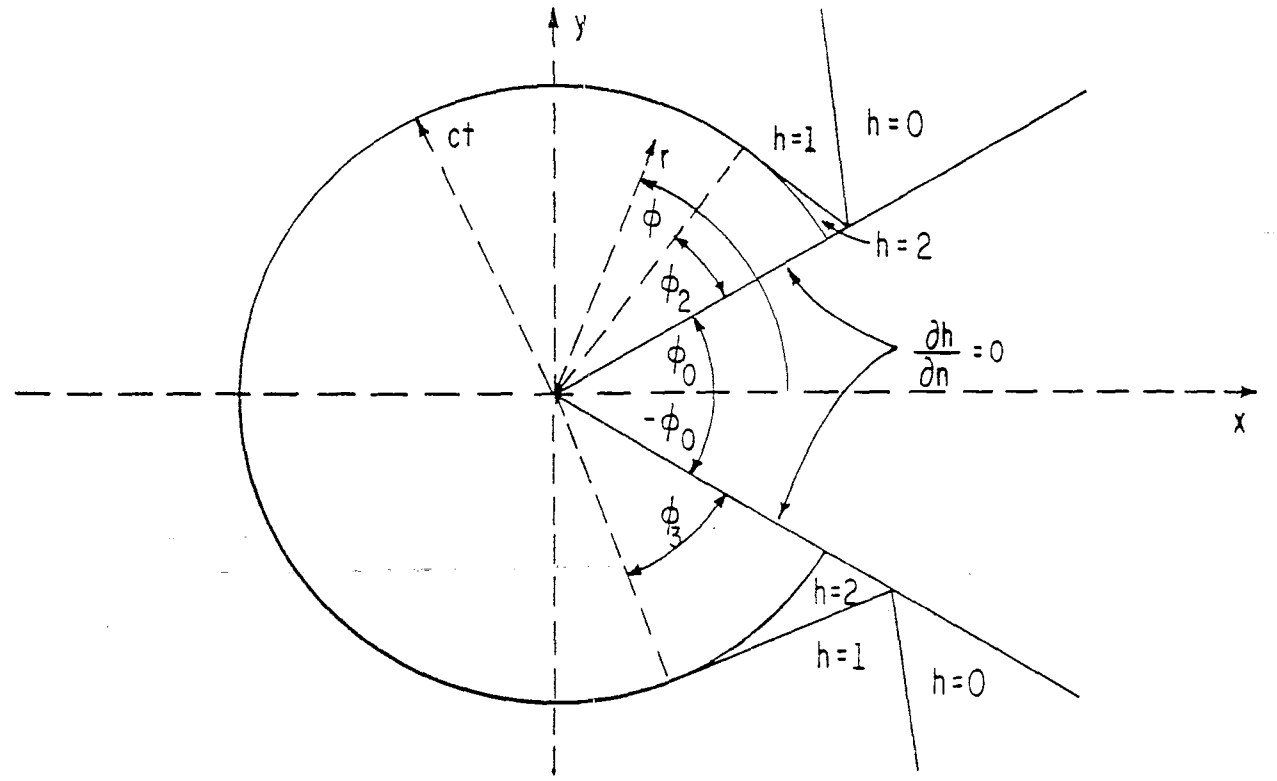

B. AFTER WAVE INCIDENCE AT EDGE: $t>0$

FIGURE 1. DIFFRACTION OF A STEP-FUNCTION WAVE AT A PERFECTLY CONDUCTING WEDGE: $0 \leq \phi_1 < \phi_0$

and

$$\phi_3 = \phi_o + \phi_1 \tag{6}$$

The single magnetic field component solves a scalar wave equation of the form

$$\nabla^2 h - \frac{1}{c^2}\frac{\partial^2 h}{\partial t^2} = 0 \tag{7}$$

We use both a cylindrical and a Cartesian coordinate system related by

$$x = r\cdot\cos(\phi) \tag{8}$$

and

$$y = r\sin(\phi) \tag{9}$$

The Laplacian is then

$$\nabla^2 h = \frac{\partial^2 h}{\partial x^2} + \frac{\partial^2 h}{\partial y^2} = \frac{1}{r}\frac{\partial}{\partial r}\left(r\frac{\partial h}{\partial r}\right) + \frac{1}{r^2}\frac{\partial^2 h}{\partial \phi^2} \tag{10}$$

Note that h is taken independent of z.

To solve for h in this circular sector note that h is a function of r/ct and not of r or t separately. Note that if r and t are both multiplied by the same factor the same wave equation and boundary conditions result. There is no special r except r = 0 in the geometry; there is no special time except t = 0. Then following the approach in reference 2 define two new coordinates as

$$p = ct\left[1 - \left(\frac{r}{ct}\right)^2\right]^{1/2} \tag{11}$$

and

$$q = \left[1 - \left(\frac{r}{ct}\right)^2\right]^{1/2} \tag{12}$$

In these coordinates equation (7) becomes

$$\frac{\partial}{\partial p}\left(p^2\frac{\partial h}{\partial p}\right) - \frac{\partial}{\partial q}\left([q^2-1]\frac{\partial h}{\partial q}\right) - \frac{1}{q^2-1}\frac{\partial^2 h}{\partial \phi^2} = 0 \tag{13}$$

However, since h is only a function of ϕ and r/ct, then it is independent of p giving

$$\frac{\partial}{\partial q}\left([q^2-1]\,\frac{\partial h}{\partial q}\right) + \frac{1}{q^2-1}\,\frac{\partial^2 h}{\partial \phi^2} = 0 \tag{14}$$

Next substitute ρ for q where

$$\rho = \left(\frac{q-1}{q+1}\right)^{1/2} = \left\{\frac{ct}{r} + \left[\left(\frac{ct}{r}\right)^2 - 1\right]^{1/2}\right\}^{-1} \tag{15}$$

Equation (14) then becomes

$$\frac{1}{\rho}\frac{\partial}{\partial \rho}\left(\rho\,\frac{\partial h}{\partial \rho}\right) + \frac{1}{\rho^2}\,\frac{\partial^2 h}{\partial \phi^2} = 0 \tag{16}$$

Note that this is the Laplace equation in a special (ρ,ϕ) cylindrical coordinate system where ρ is mathematically the "radius" even though it contains both r and t.

In this special cylindrical coordinate system the circular sector of interest has $\rho = 0$ at the center ($r = 0$) and $\rho = 1$ on the circle ($r = ct$). Using equations (1) through (6) for the boundary conditions then we can obtain h as a solution of the Laplace equation (in ρ and ϕ) in the circular sector. Following Keller and Blank use a conformal transformation of the form

$$w = Re^{j\omega} = \left(e^{-j\phi_o}\,\rho\,e^{j\phi}\right)^{\lambda} \tag{17}$$

where

$$\lambda = \frac{1}{2}\left[1 - \frac{\phi_o}{\pi}\right]^{-1} \tag{18}$$

This transformation maps the circular sector onto a semicircle of radius, R = 1, in the upper w half plane. The solution of the Laplace equation can then be treated as an image problem so that we have h specified on the circumference of a full circle. Using another conformal transformation we have the solution for $\rho \le 1$ or $r \le ct$, which we call h_b, as

$$h_b = 1 + \frac{1}{\pi}\arctan\left\{\frac{-(1-\rho^{2\lambda})\cos\left(\lambda\,(\pi-\phi_1)\right)}{(1+\rho^{2\lambda})\sin\left(\lambda(\pi-\phi_1)\right)-2\rho^{\lambda}\sin(\lambda(\pi-\phi))}\right\}$$

$$+ \frac{1}{\pi}\arctan\left\{\frac{-(1-\rho^{2\lambda})\cos\left(\lambda(\pi+\phi_1)\right)}{(1+\rho^{2\lambda})\sin\left(\lambda(\pi+\phi_1)\right) + 2\rho^{\lambda}\sin(\lambda(\pi-\phi))}\right\} \tag{19}$$

where the values of the arctangents are taken between 0 and π. For further details of this solution see reference 2.

III. Diffraction at a Bend in a Perfectly Conducting Planar Sheet

Now set $\phi_1 = 0$. Due to the symmetry in the electromagnetic fields a conducting sheet can now be placed at $\phi = \pi$ without disturbing the field distribution and the results of the previous section still apply. Thus, we have the solution for an electromagnetic plane wave propagating along a conducting sheet and incident on a bend of angle, ϕ_o, as illustrated in figure 2. Equation (19) for the magnetic field in the circular sector, which includes the bend, becomes

$$h_b = 1 + \frac{1}{\pi}\arctan\left\{\frac{-(1-\rho^{2\lambda})\cos(\lambda\pi)}{(1+\rho^{2\lambda})\sin(\lambda\pi) - 2\rho^{\lambda}\sin(\lambda(\pi-\phi))}\right\}$$

$$+ \frac{1}{\pi}\arctan\left\{\frac{-(1-\rho^{2\lambda})\cos(\lambda\pi)}{(1+\rho^{2\lambda})\sin(\lambda\pi) + 2\rho^{\lambda}\sin(\lambda(\pi-\phi))}\right\} \qquad (20)$$

Using a formula for adding arctangents of the form

$$\arctan(z_1) + \arctan(z_2) = \arctan\left(\frac{z_1+z_2}{1-z_1z_2}\right) \qquad (21)$$

then equation (20) becomes

$$h_b = 1 + \frac{1}{\pi}\arctan\left\{\frac{-2(1-\rho^{2\lambda})\cos(\lambda\pi)(1+\rho^{2\lambda})\sin(\lambda\pi)}{(1+\rho^{2\lambda})^2\sin^2(\lambda\pi) - 4\rho^{2\lambda}\sin^2(\lambda(\pi-\phi)) - (1-\rho^{2\lambda})^2\cos^2(\lambda\pi)}\right\}$$

$$= 1 + \frac{1}{\pi}\arctan\left\{\frac{(1-\rho^{4\lambda})\sin(2\lambda\pi)}{(1+\rho^{4\lambda})\cos(2\lambda\pi) - 2\rho^{2\lambda}\cos(2\lambda(\pi-\phi))}\right\} \qquad (22)$$

For convenience shift the argument of the trigonometric functions in equation (22) by π giving

$$h_b = 1 + \frac{1}{\pi}\arctan\left\{\frac{(1-\rho^{4\lambda})\sin((2\lambda-1)\pi)}{(1+\rho^{4\lambda})\cos((2\lambda-1)\pi) - 2\rho^{2\lambda}\cos((2\lambda-1)\pi - 2\lambda\phi)}\right\} \qquad (23)$$

The arctangent is taken between 0 and π. One interesting case from this result is the limiting case for large t (or small ρ) giving

$$\lim_{t\to\infty} h_b = 1 + \frac{1}{\pi}\arctan\left\{\tan((2\lambda-1)\pi)\right\} = \left[1 - \frac{\phi_o}{\pi}\right]^{-1} \qquad (24)$$

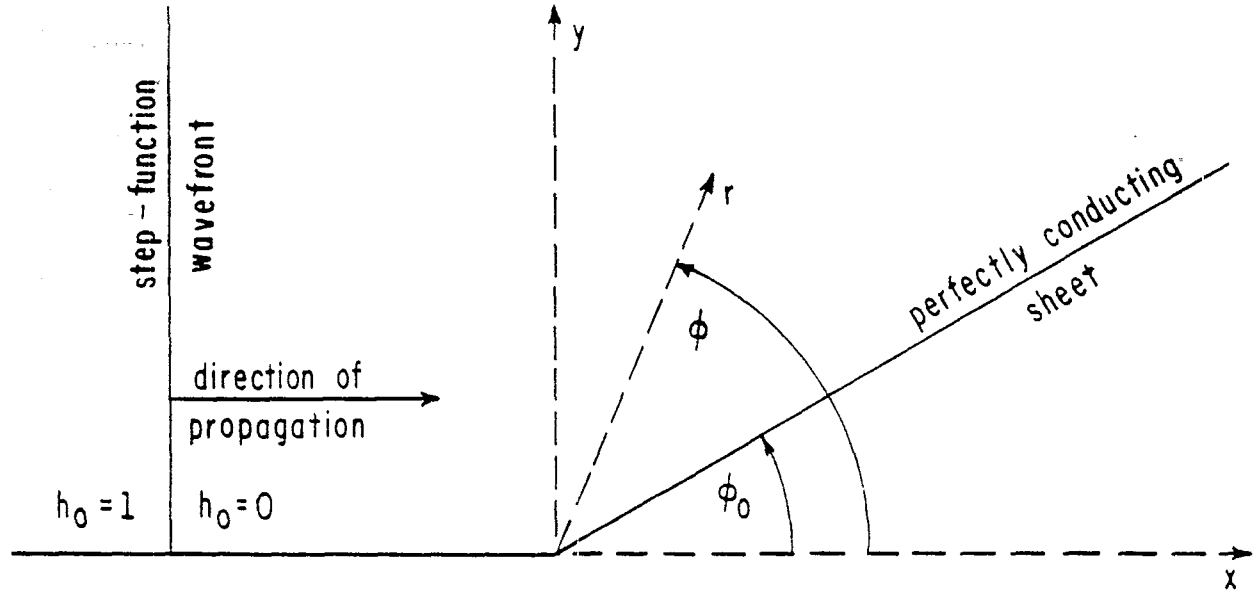

A. BEFORE WAVE INCIDENCE AT BEND: $t < 0$

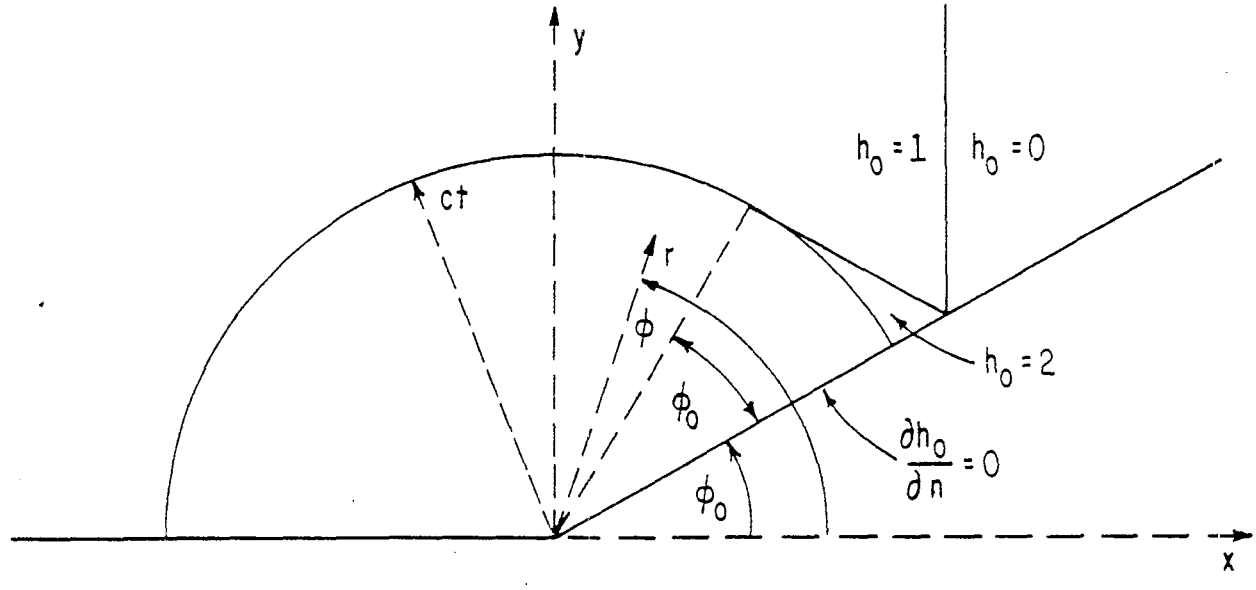

B. AFTER WAVE INCIDENCE AT BEND: $t > 0$

FIGURE 2. DIFFRACTION OF A STEP-FUNCTION WAVE AT A BEND IN A PERFECTLY CONDUCTING SHEET: $\phi_1 = 0$

Now define a normalized time as

$$\tau \equiv \frac{t - \frac{x}{c}}{\frac{r}{c}} = \frac{ct}{r} - \cos(\phi) \tag{25}$$

The initial rise of the magnetic field for an observer at r is at $\tau=0$. In calculating the waveforms there are two cases of interest. First, let $\phi_o < \phi < 2\phi_o$. Then for $\tau<0$

$$h_o = 0 \tag{26}$$

for $0 \leq \tau < \cos(2\phi_o - \phi) - \cos(\phi)$

$$h_o = 1 \tag{27}$$

for $\cos(2\phi_o - \phi) - \cos(\phi) \leq \tau \leq 1 - \cos(\phi)$

$$h_o = 2 \tag{28}$$

and for $1 - \cos(\phi) \leq \tau$

$$h_o = h_b \tag{29}$$

Second, let $2\phi_o < \phi \leq \pi$. Then for $\tau < 0$

$$h_o = 0 \tag{30}$$

for $0 \leq \tau \leq 1 - \cos(\phi)$

$$h_o = 1 \tag{31}$$

and for $1 - \cos(\phi) \leq \tau$

$$h_o = h_b \tag{32}$$

To solve for the electric field components use one of Maxwell's equations as

$$\nabla \times \vec{H} = \varepsilon \frac{\partial \vec{E}}{\partial t} \tag{33}$$

Now set

$$\vec{H} \equiv H_o \vec{h}_o \tag{34}$$

and

$$\vec{E} \equiv \sqrt{\frac{\mu}{\varepsilon}} H_o \vec{e}_o \tag{35}$$

where we also have

$$c = \frac{1}{\sqrt{\mu\varepsilon}} \tag{36}$$

Then the curl equation becomes

$$\nabla \times \vec{h}_o = \frac{\partial \vec{e}_o}{\partial (ct)} \tag{37}$$

The normalized magnetic field is

$$\vec{h}_o = h_o \vec{e}_z \tag{38}$$

and the normalized electric field is

$$\vec{e}_o = e_{o_x} \vec{e}_x + e_{o_y} \vec{e}_y = e_{o_r} \vec{e}_r + e_{o_\phi} \vec{e}_\phi \tag{39}$$

where $\vec{e}_x$, $\vec{e}_y$, $\vec{e}_z$, $\vec{e}_r$, and $\vec{e}_\phi$ are unit vectors for the directions indicated by the subscripts.

Since the field components can be expressed as functions of τ and ϕ we can write the curl equation

$$\frac{\partial \vec{e}_o}{\partial \tau} = r \nabla \times \vec{h}_o \tag{40}$$

which can be expanded in cylindrical coordinates as

$$\frac{\partial e_{o_r}}{\partial \tau} = \frac{\partial h_o}{\partial \phi} \tag{41}$$

and

$$\frac{\partial e_{o_\phi}}{\partial \tau} = -r\frac{\partial h_o}{\partial r} = -\left(r\frac{\partial \rho}{\partial r}\right)\frac{\partial h_o}{\partial \rho} \tag{42}$$

From equation (15) we calculate

$$r\,\frac{\partial \rho}{\partial r} = \rho\,\frac{ct}{r}\left[\left(\frac{ct}{r}\right)^2 - 1\right]^{-\frac{1}{2}}$$

which is used in equation (42). From equation (23) we calculate

$$\frac{\partial h_b}{\partial \rho} = \frac{1}{\pi}\left\{1 + \left[\frac{(1-\rho^{4\lambda})\,\sin((2\lambda-1)\pi)}{(1+\rho^{4\lambda})\,\cos((2\lambda-1)\pi) - 2\rho^{2\lambda}\,\cos((2\lambda-1)\pi - 2\lambda\phi)}\right]^2\right\}^{-1}$$

$$\cdot\frac{\left\{\begin{array}{l} -4\lambda\rho^{4\lambda-1}\,\sin((2\lambda-1)\pi)\left[(1+\rho^{4\lambda})\,\cos((2\lambda-1)\pi) - 2\rho^{2\lambda}\,\cos((2\lambda-1)\pi - 2\lambda\phi)\right] \\ -(1-\rho^{4\lambda})\,\sin((2\lambda-1)\pi)\left[4\lambda\rho^{4\lambda-1}\,\cos((2\lambda-1)\pi) - 4\lambda\rho^{2\lambda-1}\,\cos((2\lambda-1)\pi - 2\lambda\phi)\right] \end{array}\right\}}{\left[(1+\rho^{4\lambda})\,\cos((2\lambda-1)\pi) - 2\rho^{2\lambda}\,\cos((2\lambda-1)\pi - 2\lambda\phi)\right]^2} \tag{44}$$

and

$$\frac{\partial h_b}{\partial \phi} = \frac{1}{\pi}\left\{1 + \left[\frac{(1-\rho^{4\lambda})\,\sin((2\lambda-1)\pi)}{(1+\rho^{4\lambda})\,\cos((2\lambda-1)\pi) - 2\rho^{2\lambda}\,\cos((2\lambda-1)\,\pi - 2\lambda\phi)}\right]^2\right\}^{-1}$$

$$\cdot\left\{\frac{(1-\rho^{4\lambda})\,\sin((2\lambda-1)\pi)}{\left[(1+\rho^{4\lambda})\,\cos((2\lambda-1)\pi) - 2\rho^{2\lambda}\,\cos((2\lambda-1)\pi - 2\lambda\phi)\right]^2}\right\} \cdot 4\lambda\rho^{2\lambda}\,\sin((2\lambda-1)\pi - 2\lambda\phi) \tag{45}$$

Substituting these expressions in equations (41) and (42) the cylindrical components of the normalized electric field can be obtained in terms of an integral over the normalized time. The Cartesian components can then be obtained from

$$e_{o_x} = e_{o_r} \cos(\phi) - e_{o_\phi} \sin(\phi) \tag{46}$$

and

$$e_{o_y} = e_{o_r} \sin(\phi) + e_{o_\phi} \cos(\phi) \tag{47}$$

Equations (41) and (42) are used to obtain the normalized electric field for $r < ct$. For $r > ct$ the normalized electric field is somewhat simpler; it can be calculated by considering only the incident wave and the reflection of the incident wave from the conducting sheet at $\phi=\phi_o$ under the assumption that this is an infinite conducting plane. As with the magnetic field in equations (26) through (32), there are two cases of interest for calculating the waveforms. First, let $\phi_o < \phi < 2\phi_o$.
Then for $\tau < 0$

$$e_{o_y} = 0 \tag{48}$$

and

$$e_{o_x} = 0 \tag{49}$$

for $0 \leq \tau < \cos(2\phi_o-\phi) - \cos(\phi)$

$$e_{o_y} = 1 \tag{50}$$

and

$$e_{o_x} = 0 \tag{51}$$

for $\cos(2\phi_o-\phi) - \cos(\phi) \leq \tau \leq 1-\cos(\phi)$

$$e_{o_y} = 1 + \cos(2\phi_o) \tag{52}$$

and

$$e_{o_x} = -\sin(2\phi_o) \tag{53}$$

and for $1 - \cos(\phi) \leq \tau$

$$e_{o_r} = \left[1+\cos(2\phi_o)\right] \sin(\phi) - \sin(2\phi_o) \cos(\phi) + \int_{1-\cos(\phi)}^{\tau} \frac{\partial h_b}{\partial \phi} d\tau' \tag{54}$$

and

$$e_{o_\phi} = \sin(2\phi_o)\,\sin\phi + \left[1+\cos(2\phi_o)\right]\cos(\phi) - \int_{1-\cos(\phi)}^{\tau} \left(r\frac{\partial\rho}{\partial r}\right)\frac{\partial h_b}{\partial\rho}\,d\tau' \qquad (55)$$

Second, let $2\phi_o < \phi \leq \pi$. Then for $\tau < 0$

$$e_{o_y} = 0 \qquad (56)$$

and

$$e_{o_x} = 0 \qquad (57)$$

for $0 \leq \tau \leq 1 - \cos(\phi)$

$$e_{o_y} = 1 \qquad (58)$$

and

$$e_{o_x} = 0 \qquad (59)$$

and for $1 - \cos(\phi) \leq \tau$

$$e_{o_r} = \sin(\phi) + \int_{1-\cos(\phi)}^{\tau} \frac{\partial h_b}{\partial\phi}\,d\tau' \qquad (60)$$

and

$$e_{o_\phi} = \cos(\phi) - \int_{1-\cos(\phi)}^{\tau} \left(r\frac{\partial\rho}{\partial r}\right)\frac{\partial h_b}{\partial\rho}\,d\tau' \qquad (61)$$

For $\phi=\phi_o$ and $\phi=2\phi_o$ both the normalized electric and magnetic fields can be calculated by taking the appropriate limits in the appropriate foregoing equations.

There are limiting forms for large τ for the normalized electric field components. Note first that the limit of large τ is the same as the limit of small ρ. At $\rho=0$, the position of the bend, there can be no electric field because the electric field can have no component parallel to a perfectly conducting surface. As long as we restrict $0 < \phi_o < \pi$ then any nonzero electric field at $\rho=0$ would have a component parallel to a perfect conductor because of the two orientations of the conducting sheets which intersect at $\rho=0$. Thus we have

$$\lim_{\tau\to\infty} e_{o_r} = \lim_{\tau\to\infty} e_{o_\phi} = 0 \tag{62}$$

Furthermore, we can obtain approximate forms for the normalized electric field components for large τ. Consider the derivatives of h_b in equations (44) and (45), together with equation (43) in the limit of small ρ or large ct/r. Define

$$\tau'' \equiv \frac{ct}{r} \tag{63}$$

Then for $|\rho| \ll 1$ or $|\tau''| \gg 1$ equation (43) is

$$r\frac{\partial\rho}{\partial r} \simeq \rho \simeq \frac{1}{2\tau''} \tag{64}$$

equation (44) is

$$\frac{\partial h_b}{\partial \rho} \simeq \frac{1}{\pi}\left\{1 + \tan^2((2\lambda-1)\pi)\right\}^{-1} \cdot \frac{4\lambda\rho^{2\lambda-1}\sin((2\lambda-1)\pi)\cos((2\lambda-1)\pi-2\lambda\phi)}{\cos^2((2\lambda-1)\pi)} = \tag{65}$$

$$\frac{4\lambda}{\pi}\rho^{2\lambda-1}\sin((2\lambda-1)\pi)\cos((2\lambda-1)\pi-2\lambda\phi) \simeq \frac{4\lambda}{\pi}(2\tau'')^{1-2\lambda}\sin((2\lambda-1)\pi)\cos((2\lambda-1)\pi-2\lambda\phi)$$

and equation (45) is

$$\frac{\partial h_b}{\partial \phi} \simeq \frac{1}{\pi}\left\{1 + \tan^2((2\lambda-1)\pi)\right\}^{-1} \frac{\sin((2\lambda-1)\pi)}{\cos^2((2\lambda-1)\pi)} \cdot 4\lambda\rho^{2\lambda}\sin((2\lambda-1)\pi-2\lambda\phi) = \tag{66}$$

$$\frac{4\lambda}{\pi}\rho^{2\lambda}\sin((2\lambda-1)\pi)\sin((2\lambda-1)\pi-2\lambda\phi) \simeq \frac{4\lambda}{\pi}(2\tau'')^{-2\lambda}\sin((2\lambda-1)\pi)\sin((2\lambda-1)\pi-2\lambda\phi)$$

For large τ'' equations (41) and (42) then become

$$\frac{\partial e_{o_r}}{\partial \tau''} \simeq \frac{4\lambda}{\pi} (2\tau'')^{-2\lambda} \sin((2\lambda-1)\pi) \sin((2\lambda-1)\pi-2\lambda\phi) \tag{67}$$

and

$$\frac{\partial e_{o_\phi}}{\partial \tau''} \simeq - \frac{4\lambda}{\pi} (2\tau'')^{-2\lambda} \sin((2\lambda-1)\pi) \cos((2\lambda-1)\pi-2\lambda\phi) \tag{68}$$

Using equation (62) we can then calculate the approximate forms of the electric field components as

$$e_{o_r} = - \int_{\tau''}^{\infty} \frac{\partial e_{o_r}}{\partial \tau'} d\tau' \simeq \frac{2\lambda}{\pi} [1-2\lambda]^{-1} (2\tau'')^{1-2\lambda} \sin((2\lambda-1)\pi) \sin((2\lambda-1)\pi-2\lambda\phi) =$$

$$- \frac{1}{\phi_o} (2\tau'')^{1-2\lambda} \sin((2\lambda-1)\pi) \sin((2\lambda-1)\pi-2\lambda\phi) \tag{69}$$

and

$$e_{o_\phi} = - \int_{\tau''}^{\infty} \frac{\partial e_{o_\phi}}{\partial \tau'} d\tau' \simeq - \frac{2\lambda}{\pi} [1-2\lambda]^{-1} (2\tau'')^{1-2\lambda} \sin((2\lambda-1)\pi) \cos((2\lambda-1)\pi-2\lambda\phi) =$$

$$\frac{1}{\phi_o} (2\tau'')^{1-2\lambda} \sin((2\lambda-1)\pi) \cos((2\lambda-1)\pi-2\lambda\phi) \tag{70}$$

These last two equations are more convenient than equations (54), (55), (60), and (61) for large τ. In fact, we found it convenient in the numerical calculations to use equations (69) and (70) to calculate the electric field components for sufficiently large τ that these equations are accurate. Then for smaller τ, the values from these last two equations were used as the starting points for integrals which were run backwards in τ, using the accurate values of the derivatives in equations (43), (44), and (45).

The pulse shapes for the three normalized electromagnetic field components (h_o, e_{o_y}, and e_{o_x}) are plotted in figures 3 through 7 for five values of ϕ_o, the

angle of bend of the conducting sheet. Each figure is for a separate ϕ_o. Each graph includes curves for several values of ϕ. The maximum values of h_o, and e_{o_y} and the minimum values of e_{o_x} are summarized in figure 8 as a function of ϕ for five values of ϕ_o. As one can see, the distortion of the incident step-function waveform is minimized by making ϕ_o small. For a given ϕ_o the waveform distortion is minimized at ϕ close to π. There is a region, $\phi_o \leq \phi \leq 2\phi_o$, where the distortion of the incident waveform can be quite significant. To remove significant waveform distortion it is necessary that ϕ_o be small and ϕ be somewhat larger than $2\phi_o$. Note that in the limit of large τ the electric field components go to zero for $\phi_o > 0$. However, in applying the results of these calculations to the region near a transition between a conical and cylindrical transmission line, note that the long time limit does not apply when reflections from the edges of the conducting sheet or from other conductors can influence the waveform at the position of interest.

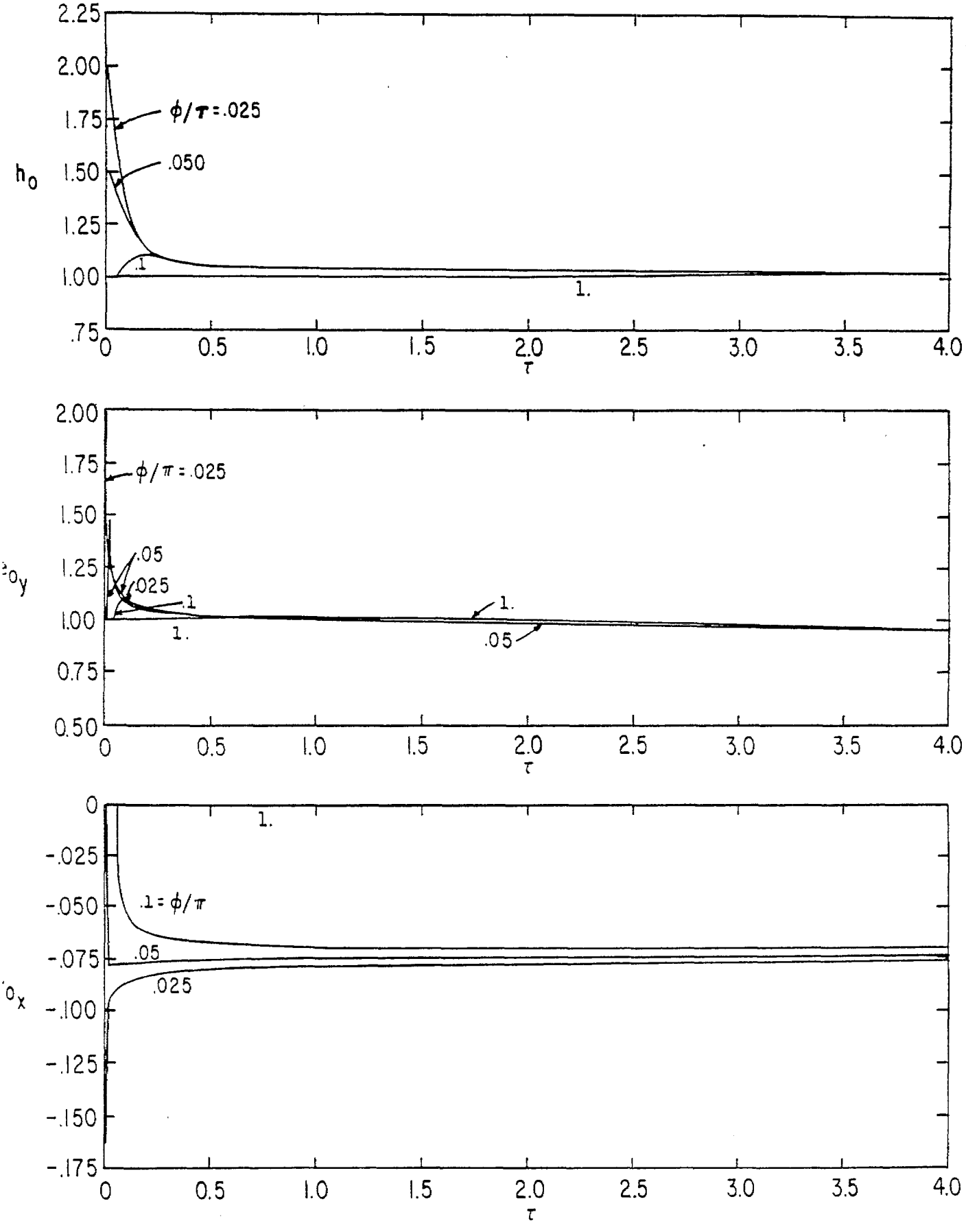

FIGURE 3. PULSE SHAPES FOR DIFFRACTION OF A STEP FUNCTION WAVE AT A BEND IN A PERFECTLY CONDUCTING SHEET: $\phi_0/\pi = .025$

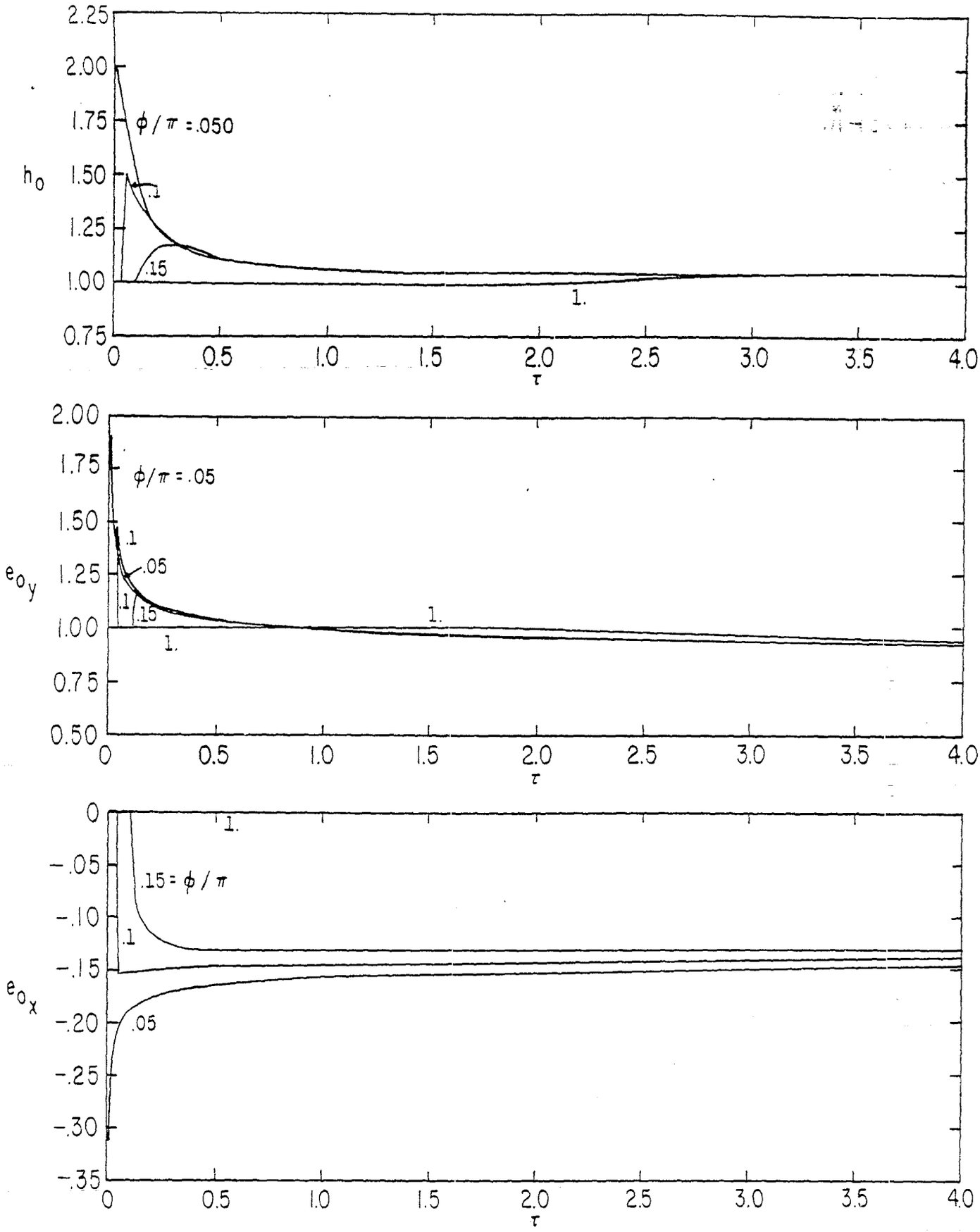

FIGURE 4. PULSE SHAPES FOR DIFFRACTION OF A STEP FUNCTION WAVE AT A BEND IN A PERFECTLY CONDUCTING SHEET: $\phi_0/\pi = .05$

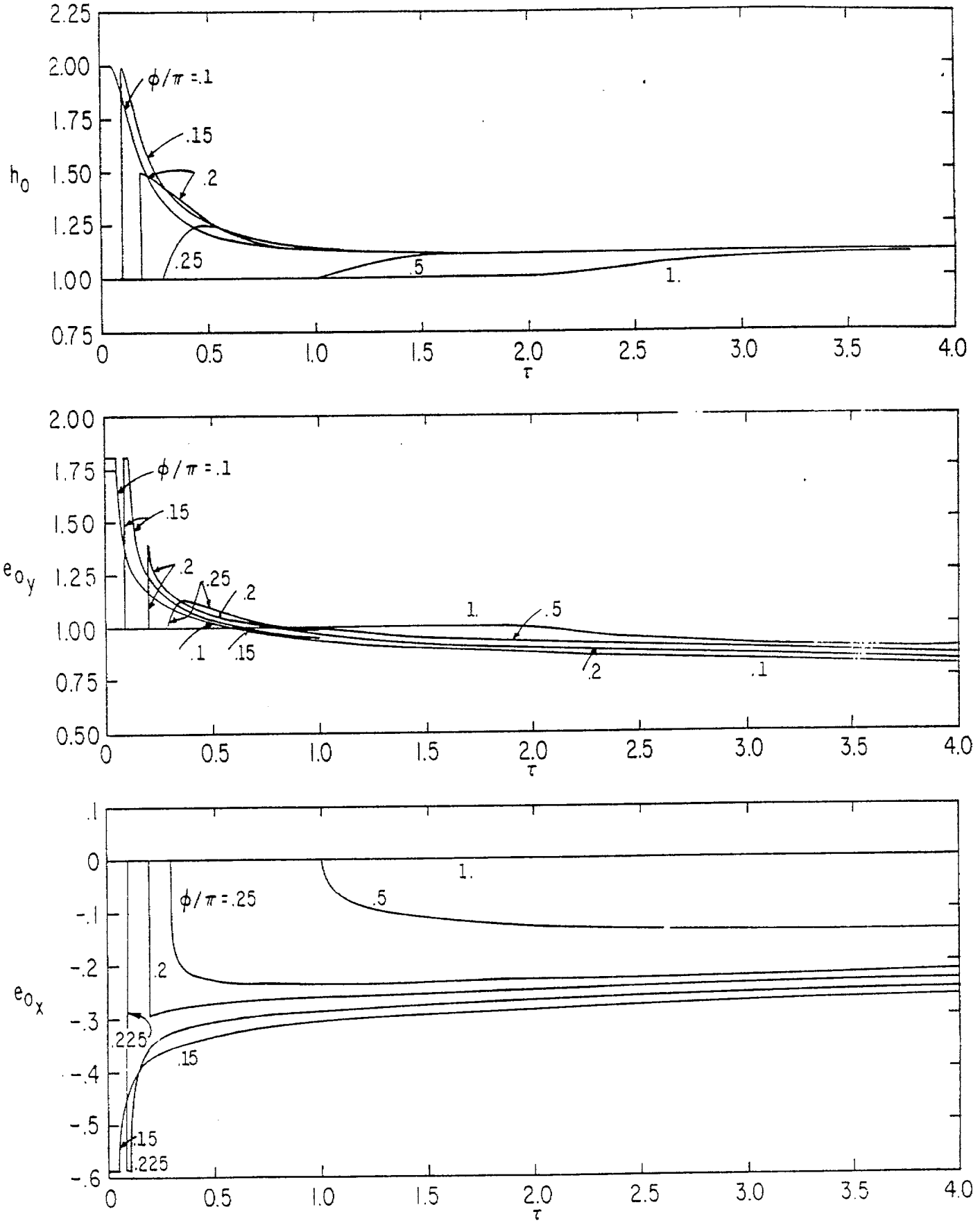

FIGURE 5. PULSE SHAPES FOR DIFFRACTION OF A STEP FUNCTION WAVE AT A BEND IN A PERFECTLY CONDUCTING SHEET: ϕ_o/π =1

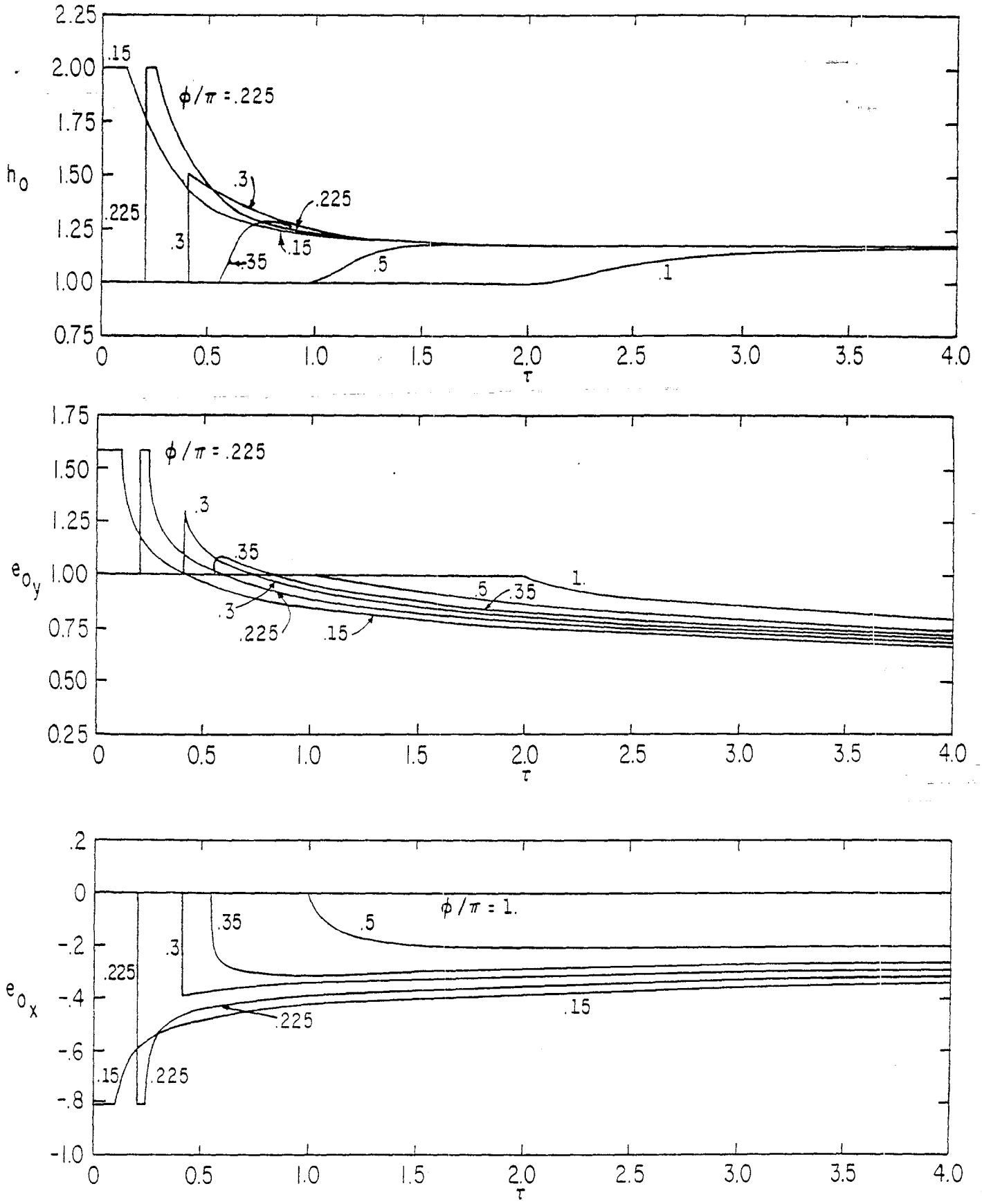

FIGURE 6. PULSE SHAPES FOR DIFFRACTION OF A STEP FUNCTION WAVE AT A BEND IN A PERFECTLY CONDUCTING SHEET: $\phi_o/\pi = .15$

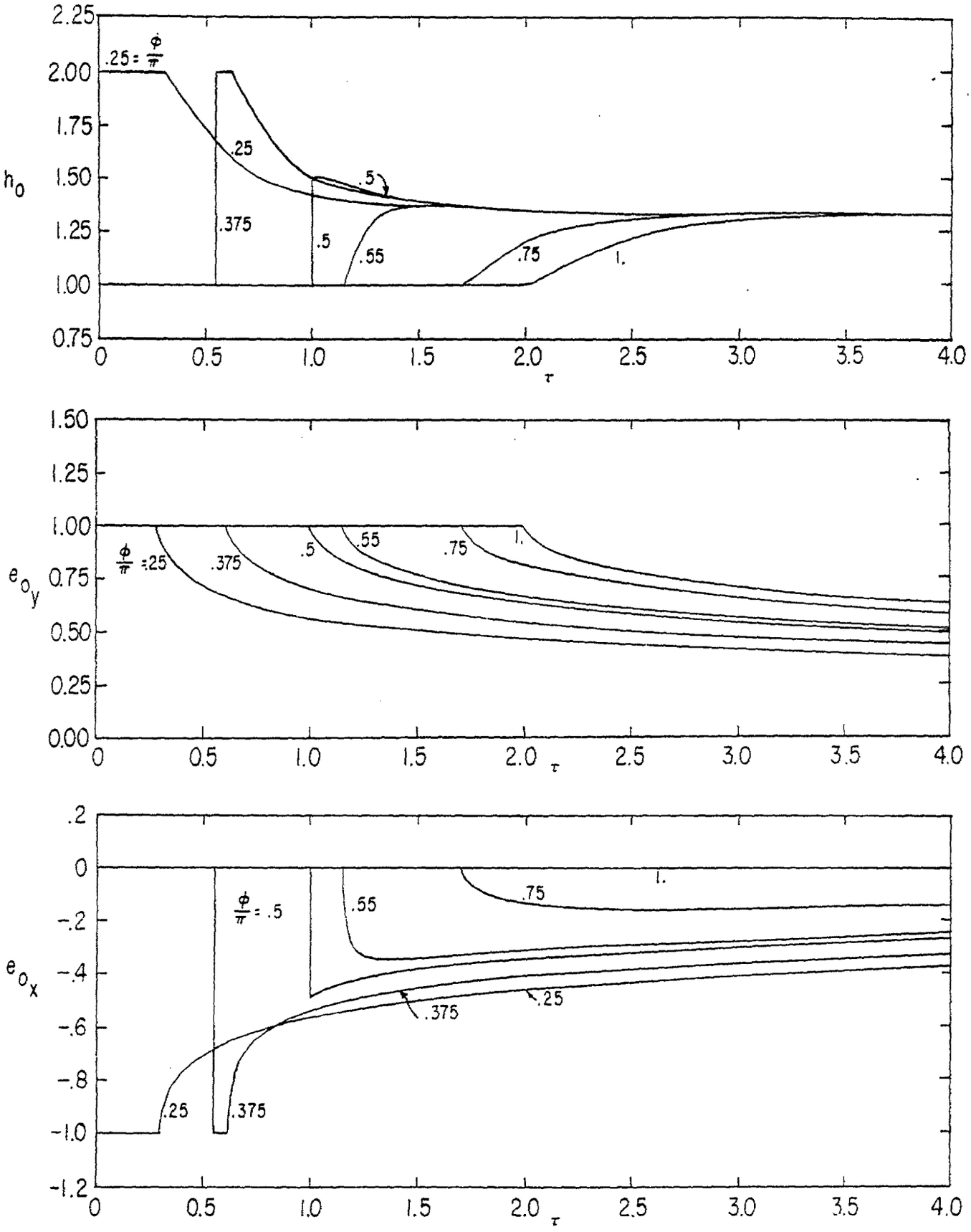

FIGURE 7. PULSE SHAPES FOR DIFFRACTION OF A STEP FUNCTION WAVE AT A BEND IN A PERFECTLY CONDUCTING SHEET: $\phi_0/\pi = .25$

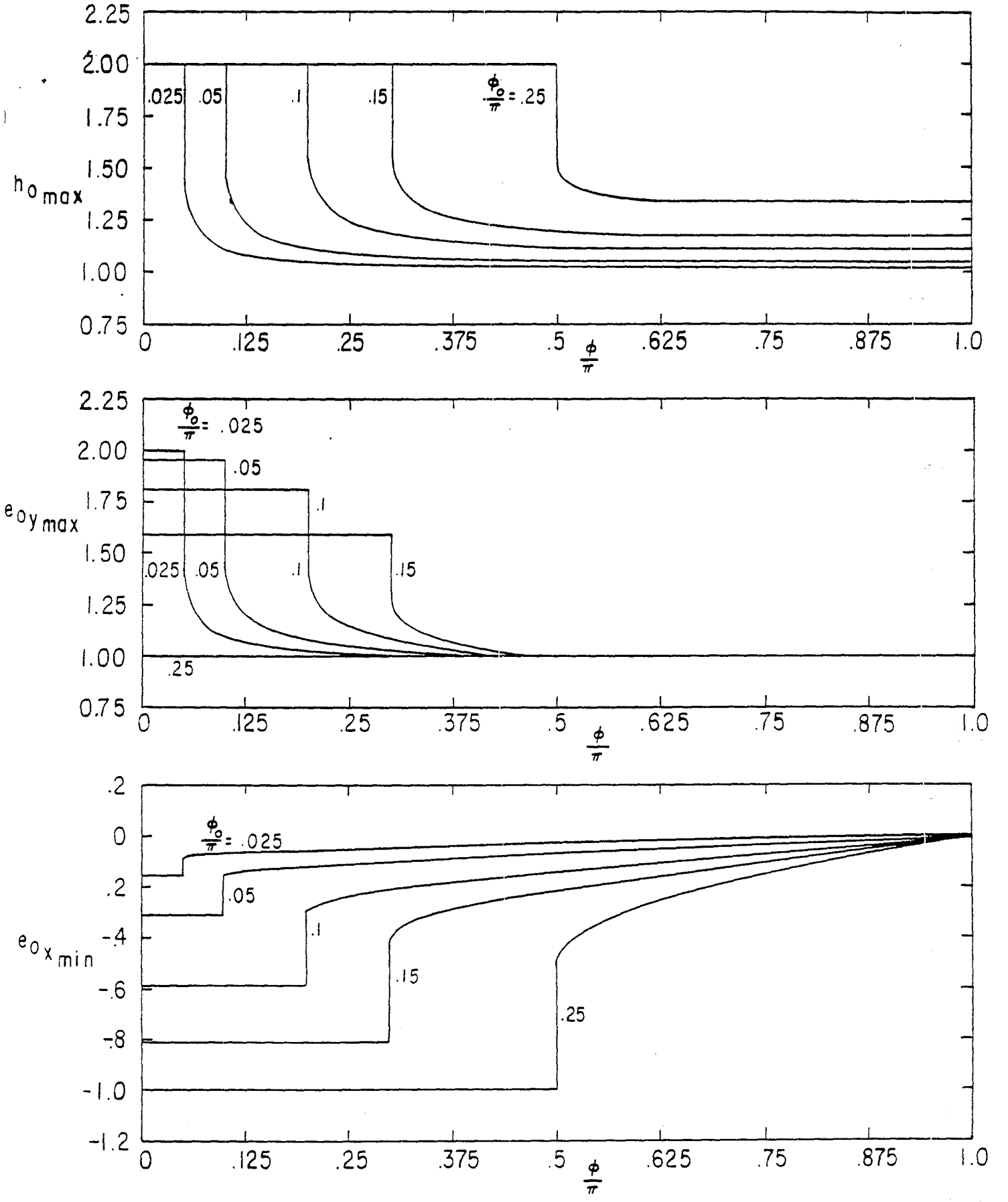

FIGURE 8. MAXIMUM OR MINIMUM VALUES OF NORMALIZED PULSE SHAPES

IV. Summary

We have calculated the diffraction of an electromagnetic plane wave at a bend in a conducting sheet where the uniform incident plane wave is propagating perpendicular to the bend and parallel to the sheet on one side of the bend. Taking first a solution for the single component of the magnetic field using the scalar wave equation, the two components of the electric field have been calculated from the magnetic field by using one of Maxwell's equations. This solution can be approximately applied to the diffraction of a wave which is transitioning from a conical to a cylindrical transmission line for times before reflections from irregularities other than the bend can influence the waveform. Note that this solution applies to conical-to-cylindrical transitions which are bends in a conducting sheet or something which approximates this.

Based on these calculations one can see the advantage of a small angle of bend, ϕ_o, in minimizing the waveform distortion. Also, the angle, ϕ, at which the waveform is observed should be somewhat larger than $2\phi_o$ for a small waveform distortion.